A proposed high-gradient laser-driven electron accelerator using crossed cylindrical laser focusing

Y. C. Huang[a) and R. L. Byer

Edward L. Ginzton Laboratory, Stanford University, Stanford, California 94305-4085

We propose a dielectric-based, crossed-laser-beam electron linear accelerator structure operating in a vacuum that is capable of providing 1 TeV electrons in approximately 1 km. The accelerator structure employs cylindrical laser focusing that allows for simplifying the fabrication process, accelerating more electrons, reducing the electron phase slip, minimizing the transverse wake-fields, and spreading the structural thermal loading. We present a 0.7 GeV/m average-gradient accelerator structure, repeated every 390 μm, subject to the laser damage fluence 2 J/cm^2 on the optical components for 100 fs laser pulses. © 1996 American Institute of Physics. [S0003-6951(96)04141-1]

With the rapid advance of laser technology, high-gradient laser-driven accelerators, primarily the laser wake-field accelerator[1,2] and the boundary-loaded vacuum linear accelerator,[3,4] have been proposed in the literature. The boundary-loaded vacuum linear accelerator, which is constructed from cascaded accelerator cells, provides a peak acceleration gradient of a few GeV s in theory. The acceleration gradient in a boundary-loaded laser-driven accelerator, like the RF accelerator gradient, is limited by damage. For 100–200 fs laser pulses, the laser damage fluence of a dielectric is on the order of 2 J/cm^2.[5,6] The corresponding surface damage field and thus the maximum electron acceleration gradient is ~10 GeV/m.

Previously we have proposed a 0.7 GeV/m average-gradient, dielectric-based, crossed-laser-beam vacuum linear accelerator[4] with integrated components on a dielectric substrate. That accelerator was axially symmetric and was limited in the ability to accelerate adequate charges for high-energy physics applications.[7] Here we proposed a similar accelerator structure employing cylindrical laser focusing that has the following desirable features: (1) It can be fabricated by using current lithographic technology; (2) the transverse wake-field vanishes;[8] (3) more electrons can be accelerated by increasing the transverse beam size; (4) the average acceleration gradient can be higher, as will be shown; (5) thermal loading can be spread over a wider area; and (6) beamstrahlung, the synchrotron radiation loss at the final electron-beam collision, can be reduced by increasing the electron beam size in one transverse direction.

Figure 1 shows the proposed crossed-laser-beam accelerator geometry, wherein an electron traverses the focal zone at an angle θ with respect to the two laser beams. The insert in Fig. 1 defines the coordinates used in this letter. The unprimed coordinate system is the laboratory frame which includes the electron velocity axis z. The primes indicate the rotated coordinates of the laser beams. The two TEM$_0$ laser beams are derived from a single laser source. They carry equal power, and are phased such that on the z axis the transverse fields in the x cancel and the longitudinal fields in the z add. The proposed accelerator structure uses repetitive

dielectric boundaries over a distance no greater than a π-phase slip between the laser field and the electron in a vacuum. Two laser beams are back-coupled from the $\pm x$ directions into the microstage using two prisms. The total internal reflection (TIR) inside the prisms permits the use of antireflective (AR) coatings for beam coupling, which are less complex than high-reflective (HR) coatings. Two HR-coated flat mirrors provide a secondary reflection and direct the two laser beams into the center of the microstage. For a small angle θ, a minimum prism size (in the z and x directions) of $2w$ is required for coupling ~90% of the laser power into the structure, where w is the Gaussian beam electrical field $1/e$ radius at the prisms. Beam clipping at the prism sets the geometrical beam coupling condition

$$3l \times \theta > w, \tag{1}$$

where l is half of the interaction length measured from the focal point. The structure is constant in the y direction and thus allows cylindrical focusing of the laser beam. The minimum drift space per microstage, where no laser fields exist, is approximately $2w$, and the total length of a microstage is $L_\mu = 2l + 2w$. The average acceleration gradient can be defined as
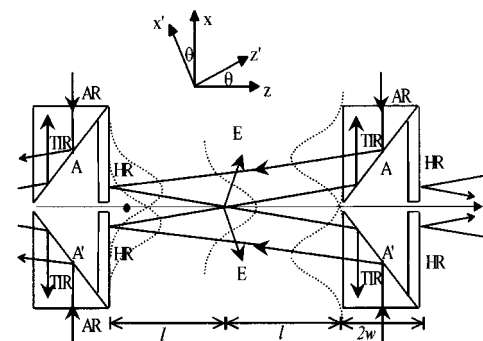
$$G = \frac{\Delta W}{L_\mu}, \tag{2}$$

FIG. 1. The schematic of a crossed-laser-beam accelerator. The electron traverses the focal zone at an angle θ with respect to each of the two beams. The two laser beams are phased such that the longitudinal fields add and the transverse fields cancel.

[a)]Electronic mail: huang@loki.stanford.edu

where ΔW is the single-stage electron energy gain.

With no variation in the y direction, the electrical field in x', $\widetilde{E}_{x'}$ in phasor notation, for a fundamental Gaussian mode is given by[9]

$$\widetilde{E}_{x'} = \left(\frac{2}{\pi}\right)^{1/4} \left(\frac{2\nu}{w(z')}P_y\right)^{1/2} \exp\left(-jkz' + j\frac{1}{2}\Phi(z')\right.$$
$$\left. -jk\frac{x'^2}{2R(z')} + j\phi\right)\exp\left(-\frac{x'^2}{w^2(z')}\right), \tag{3}$$

where $\eta = 377\ \Omega$ is the vacuum wave impedance, $w(z') = w_0\sqrt{1+(z'/z_r)^2}$ is the laser field $1/e$ radius in x', z_r is the optical Rayleigh length, P_y is the optical power per unit length in y, $k = \lambda/2\pi$ is the wave propagation constant, $\Phi(z') = \tan^{-1}(z'/z_r)$ is the Guoy phase, $R(z') = z' + z_r^2/z'$ is the radius of curvature of the wave front, and ϕ is the electron entrance phase. Compared to the spherical focusing, the Guoy phase term in Eq. (3) is reduced by a factor of 2,[10] due to the removal of the focusing from y'.

The electrical-field component in the z' can be calculated according to $\nabla'\cdot\mathbf{E} = 0$ in a vacuum. In the paraxial approximation,

$$\widetilde{E}_{z'} \approx \frac{-j}{k}\frac{\partial\widetilde{E}_{x'}}{\partial x'} = \widetilde{E}_{x'}\left(\frac{-x'}{R(z')} + 2j\frac{x'}{kw^2(z')}\right). \tag{4}$$

Assume that the electron transit aperture is small and does not noticeably affect the laser fields. The axial electric-field component in z can be summed from the two crossed laser beams by appropriate coordinate transformation. The acceleration field $E_z = \mathrm{Re}(\widetilde{E}_z)$ seen by an axial electron becomes

$$E_z = -2\left(\frac{2}{\pi}\right)^{1/4}\left(\frac{2\nu}{w_0}P_y\right)^{1/2}\theta\frac{\exp[-\hat{z}^2\hat{\theta}^2/(1+\hat{z}^2)]}{(1+\hat{z}^2)^{3/4}}$$
$$\times\cos\left(\frac{\hat{z}\hat{\theta}^2}{1+\hat{z}^2} + 1.5\tan^{-1}\hat{z}\right), \tag{5}$$

where $\hat{z}\equiv z/z_r$ is the normalized longitudinal coordinate and $\hat{\theta}\equiv\theta/(w_0/z_r)$ is the crossing angle normalized to the far-field diffraction angle w_0/z_r. In deriving Eq. (5), a minimum electron injection energy $\gamma\gg1/\theta$, a small angle $\theta\ll1$, and an electron entrance phase for maximizing E_z at $z = 0$ are assumed.

Laser damage intensity has been measured for spherical laser focusing by previous workers.[5,6] The damage power per unit length in y, $(P_y)_{\max}$, can be related to the measured damage intensity $I_{\max}$ by $(P_y)_{\max} = I_{\max}\sqrt{\pi/2}w(z=l)$, where $z = l$ is the location of the HR mirror. The axial acceleration field under the limit set by structure damage is thus

$$E_z = -2\sqrt{2\eta I_{\max}}\theta\frac{(1+\hat{l}^2)^{1/4}}{(1+\hat{z}^2)^{3/4}}\exp\left(\frac{-\hat{z}^2\hat{\theta}^2}{1+\hat{z}^2}\right)$$
$$\times\cos\left(\frac{\hat{z}\hat{\theta}^2}{1+\hat{z}^2} + 1.5\tan^{-1}\hat{z}\right), \tag{6}$$

where $\hat{l}\equiv l/z_r$ is the location of the high reflectivity mirror in z normalized to the optical Rayleigh length z_r.
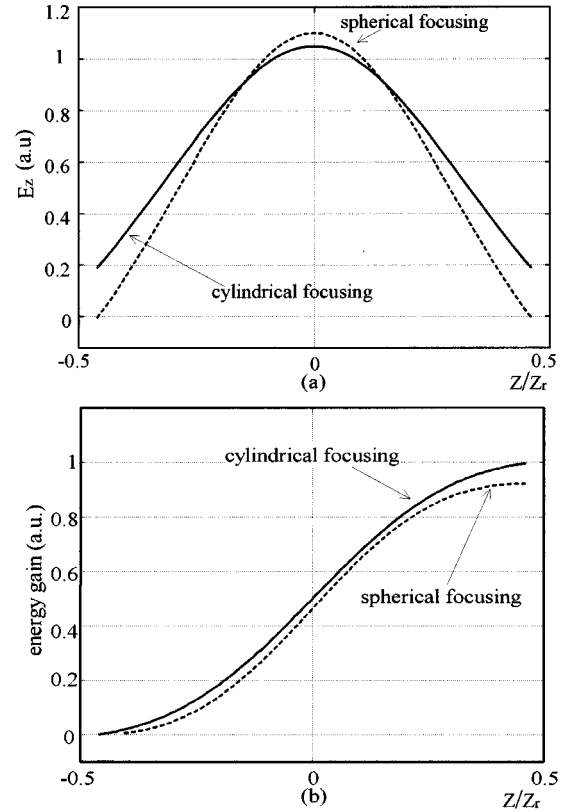

FIG. 2. (a) The normalized axial acceleration fields for cylindrical laser focusing and spherical focusing for $\hat{l} = 0.46$ and $\hat{\theta} = 1.37$. The curve for the cylindrical focusing is weaker at the focus but decreases more slowly along z. (b) Electron energy gain integrated from the two curves in (a). The single-stage energy gain for the cylindrical laser focusing scheme if ~10% higher than that for the spherical focusing under the same laser damage limit.

As a comparison, the corresponding axial acceleration field for the spherical laser focusing case can be derived from Refs. 3 and 4, yielding

$$E_z = -2\sqrt{2\eta I_{\max}}\theta\frac{(1+\hat{l}^2)^{1/2}}{(1+\hat{z}^2)}\exp\left(\frac{-\hat{z}^2\hat{\theta}^2}{1+\hat{z}^2}\right)$$
$$\times\cos\left(\frac{\hat{z}\hat{\theta}^2}{1+\hat{z}^2} + 2\tan^{-1}\hat{z}\right). \tag{7}$$

The phase slip for the cylindrical focusing case is less severe due to the removal of the 0.5 Guoy phase from the y direction. However, at the focal point $z = 0$, the axial acceleration field for the spherical laser focusing is stronger by a factor of $(1+\hat{l}^2)^{1/4}$.

Figure 2(a) shows the comparison of the axial field E_z for the two focusing schemes at $\hat{l} = 0.46$ and $\hat{\theta} = 1.37$, where the spherical focusing case gives the maximum electron energy gain.[4] The axial field for the cylindrical focusing is indeed slightly weaker at the focus but decreases more slowly along z due to the smaller phase slip. The single-stage energy gain, the area under the two curves in Fig. 2(a), is plotted in Fig. 2(b). The cylindrical focusing provides a higher single-stage energy gain, by ~10%, under the same damage fluence assumptions.

The average acceleration gradient, calculated from Eq. (2), can be evaluated as a set of contours for different inter-
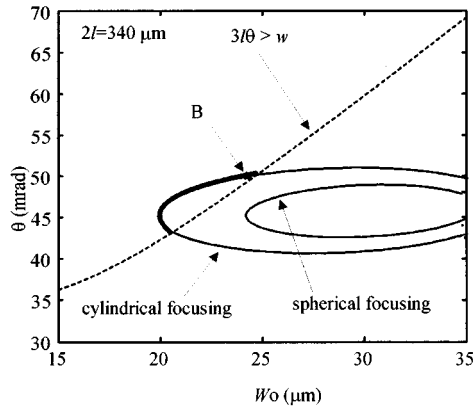
FIG. 3. 0.71 GeV/m contours for the cylindrical and spherical focusing for $2l=340$ μm. Design parameters for (θ, w_0) are allowed above the dashed line, which is governed by Eq. (1). No working (θ, w_0) pairs are obtained for the spherical focusing. Point B for the cylindrical focusing gives 0.71 GeV/m average acceleration gradient with $\theta=50$ mrad, $w_0=25\mu$m, $L_\mu =390$ μm, and single-state energy gain=280 keV.
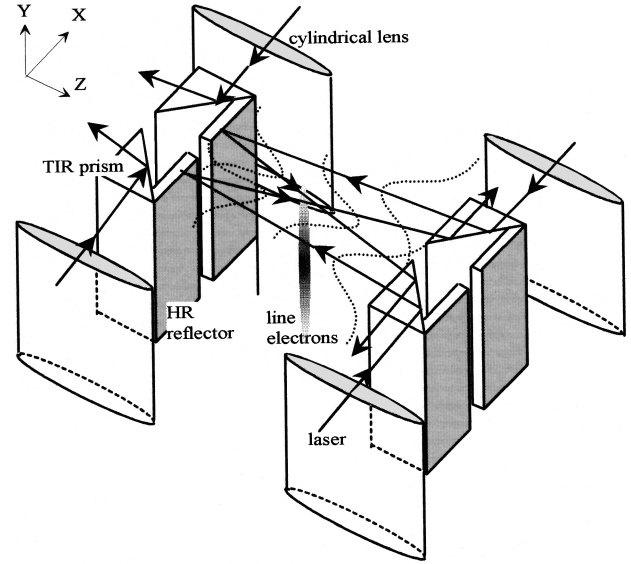

FIG. 4. The 3D view of the proposed accelerator structure. A linear charge in y is accelerated through two crossed cylindrical laser beams. The cross section of the TIR prism is 50×50 μm^2, the height can be a few hundred micrometers, and the stage length along z, including the distance occupied by the optical components, is 390 μm. The optical components can be implanted or etched into a dielectric substrate.

action length in the (θ, w_0) space. These contours, indicating an operation range of (θ, w_0), shrink as the specified average gradient increases or the interaction length increases. A large θ or a small w_0 gives more electron phase slip, while a small θ or a large w_0 (loose focusing) reduces the axial field strength. As a result a large average gradient at a constant interaction length or a long interaction length at a constant gradient, which both require small phase slip and a high axial field, reduces the available (θ, w_0) pairs.

Figure 3 shows the 0.71 GeV/m gradient contours for an interaction length of $2l=340$ μm and a laser wavelength of 1 μm for the two types of laser focusing. The boundary of Eq. (1) is overlaid as a dashed line in the same plot. Only those (θ, w_0) pairs above the dashed line, labeled by a dark solid line, satisfy the geometric coupling condition Eq. (1). It is seen in Fig. 3 that at the specified interaction length and average acceleration gradient the cylindrical focusing scheme is able to provide a range of (θ, w_0) pairs which satisfies the geometrical coupling condition, whereas this particular spherical focusing scheme provides no valid (θ, w_0) pairs for achieving the same acceleration gradient. For example, if B in Fig. 3 is chosen to be the operation point using the cylindrical laser focusing, 0.71 GeV/m average acceleration gradient can be obtained with a crossing angle $\theta=50$ mrad, a laser waist size $w_0=25$ μm, a repeat distance $L_\mu=390$ μm, and the single-stage energy gain of 280 keV.

Figure 4 shows the 3D view of the proposed microaccelerator stage which can be cascaded into a linear array for continuous electron acceleration. Modern lithographic and etching technology can provide the fabrication precision with a relatively low cost for mass production. Electro-optical phase controllers for maintaining phase coherence and cylindrical microlenses for focusing laser beams can be integrated into the same dielectric substrate in a batch process.

To transmit the electrons, an electron slit small compared to the laser waist is shown in Fig. 4. Using the numerical technique in Ref. 11, we calculated a 20% gradient reduction due to the leakage laser field through a 4 μm slit.

Following the same calculations in Ref. 7, we obtain the maximum electron density $\sim 3\times10^7$/mm in y, subject to a 10% radiation loss per accelerator stage and the 10 GV/m damage field for 100 fs laser pulses. The system parameters used in our calculation are refractive index of 1.5, electron slit width of 4 μm, electron bunch length in $z=0.03$ μm, and electron energy $\sim$1 TeV.

We have proposed a dielectric-based, cross-laser-beam, vacuum linear accelerator structure that employs cylindrical laser focusing to accelerate electrons. The cylindrical laser focusing scheme is superior in terms of simplifying the fabrication process, achieving a higher average acceleration gradient, spreading structure thermal loading, increasing the beam current, minimizing the transverse wake field, and reducing the synchrotron radiation loss. A sub-GeV/m average acceleration gradient, subject to 2 J/cm^2 laser damage fluence for 100 fs laser pulses, is achievable in the proposed accelerator structure with a stage repeat distance of 390 μm.

[1] T. Tajima and J. M. Dawson, Phys. Rev. Lett. **43**, 267 (1979).

[2] C. E. Clayton, K. A. Marsh, A. Dyson, M. Everett, A. Lal, W. P. Leemans, R. Williams, and C. Joshi, Phys. Rev. Lett. **70**, 37 (1993).

[3] P. Sprangle, E. Esarey, J. Krall, and A. Ting, Opt. Commun. **124**, 69 (1996).

[4] Y. C. Huang, D. Zheng, W. M. Tulloch, and R. L. Byer, Appl. Phys. Lett. **68**, 753 (1996).

[5] B. C. Stuart, M. D. Feit, A. M. Rubenchik, B. W. Shore, and M. D. Perry, Phys. Rev. Lett. **74**, 2248 (1995).

[6] D. von der Linde and H. Schuler, J. Opt. Soc. Am. B **13**, 216 (1996).

[7] P. Sprangle, E. Esarey, and J. Krall, Phys. Plasmas **3**, 2183 (1996).

[8] A. Tremaine and J. Rosenzweig (unpublished).

[9] A. E. Siegman, *Lasers* (University Science Books, Mill Valley, CA, 1986), p. 646.

[10] A. E. Siegman, *Lasers* (University Science Books, Mill Valley, CA, 1986), p. 664.

[11] J. A. Edighoffer and R. H. Pantell, J. Appl. Phys. **50**, 6120 (1979).